BIOCHEMISTRY
including biophysical chemistry & molecular biology

Article

pubs.acs.org/biochemistry

Detection of Labile Low-Molecular-Mass Transition Metal Complexes in Mitochondria

Sean P. McCormick,[†] Michael J. Moore,[†] and Paul A. Lindahl*[,†,‡]

[†]Department of Chemistry, Texas A&M University, College Station, Texas 77843-3255, United States

[‡]Department of Biochemistry and Biophysics, Texas A&M University, College Station, Texas 77843-2128, United States

Supporting Information

ABSTRACT: Liquid chromatography was used with an online inductively coupled plasma mass spectrometer to detect low-molecular-mass (LMM) transition metal complexes in mitochondria isolated from fermenting yeast cells, human Jurkat cells, and mouse brain and liver. These complexes constituted 20−40% of total mitochondrial Mn, Fe, Zn, and Cu ions. The major LMM Mn complex in yeast mitochondria, called Mn_{1100}, had a mass of ∼1100 Da and a concentration of ∼2 μM. Mammalian mitochondria contained a second Mn species with a mass of ∼2000 Da at a comparable concentration. The major Fe complex in mitochondria isolated from exponentially growing yeast cells had a mass of ∼580 Da; the concentration of Fe_{580} in mitochondria was ∼100 μM. When mitochondria were isolated from fermenting cells in postexponential phase, the mass of the dominant LMM Fe complex was ∼1100 Da. Upon incubation, the intensity of Fe_{1100} declined and that of Fe_{580} increased, suggesting that the two are interrelated. Mammalian mitochondria contained Fe_{580} and two other Fe species (Fe_{2000} and Fe_{1100}) at concentrations of ∼50 μM each. The dominant LMM Zn species in mitochondria had a mass of ∼1200 Da and a concentration of ∼110 μM. Mammalian mitochondria contained a second major LMM Zn species at 1500 Da. The dominant LMM Cu species in yeast mitochondria had a mass of ∼5000 Da and a concentration in yeast mitochondria of ∼16 μM; Cu_{5000} was not observed in mammalian mitochondria. The dominant Co species in mitochondria, Co_{1200}, had a concentration of 20 nM and was probably a cobalamin. Mammalian but not yeast mitochondria contained a LMM Mo species, Mo_{730}, at a concentration of ∼1 μM. Increasing Mn, Fe, Cu, and Zn concentrations 10-fold in the medium increased the concentration of the same element in the corresponding isolated mitochondria. Treatment with metal chelators confirmed that these LMM species were labile. The dominant S species at 1100 Da was not free glutathione or glutathione disulfide.

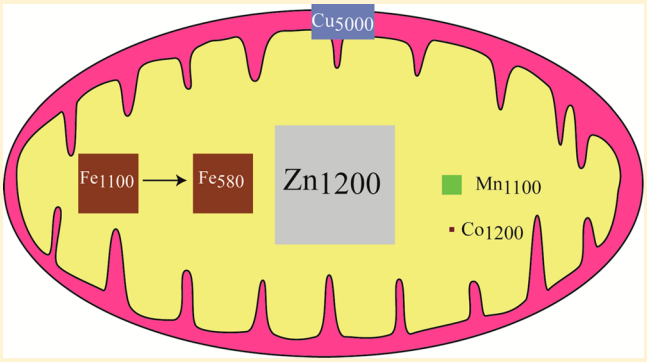

Many transition metal complexes are labile, meaning that their coordinating ligands are weakly bound and rapidly exchanging with other ligands in solution. This behavior adds a significant challenge to the isolation, identification, and characterization of such labile metal pools (LMPs) in cells.[1] These pools have been detected by incubating live intact cells with custom-designed fluorescence-based chelators, also known as sensors or probes.[2] Chelator probes penetrate cell membranes and coordinate the metal ions that compose such pools; they can also be targeted to specific organelles within the cell. Binding metal ions either enhances or quenches the fluorescence properties of the probes, thereby reporting on the existence and size of such pools.

The use of chelator probes has dramatically improved our awareness of LMPs in cells, yet many details, including the composition, structure, and function of the metal pools, remain unknown. LMPs likely participate in metal ion trafficking, regulation, signaling, and storage and release. Such processes require that metals coordinate ligands weakly enough such that the metals can be transferred from one species to another, or that the metals can dynamically bind to regulatory sites in a concentration-sensitive manner. These processes play vital roles in metal ion metabolism and are often altered in metal-associated diseases. These considerations motivate our efforts to identify and characterize LMPs, the challenges associated with their lability notwithstanding.

The benefits of detecting LMPs in live intact cells and organelles using fluorescence-based probes are counterbalanced by the fact that the sought-after complexes are destroyed during detection; i.e., the endogenous ligands associated with LMPs dissociate when the probe coordinates the metal. This is a major disadvantage because the ligand environment dictates many properties of these complexes. Also, the binding strength required to chelate a particular metal ion pool is unknown, such that stronger probes might overestimate the size of a pool and weaker ones might underestimate it. LMPs may be

Received: December 19, 2014
Revised: April 20, 2015
Published: May 27, 2015

DOI: 10.1021/bi5015437
Biochemistry 2015, 54, 3442−3453

heterogeneous, with more than one metal complex contributing. Probes are often championed as being specific for a particular metal ion, but they actually need to be specific for a particular metal ion complex, a far more difficult requirement. Deciphering the molecular-level function of each complex that composes a heterogeneous LMP based solely on the overall chelation properties of the pool seems virtually impossible.

Ligand-exchange rates of LMPs are likely to be fast, but if they were faster than the rates of relevant biochemical reactions, e.g., binding of a complex to a receptor, the complexes would lack a defined shape, a requirement of receptor recognition. With such extreme fluxionality, how could cells use such complexes in trafficking, regulation, signaling, or storage? Would not their coordination sites become available for deleterious Fenton and Haber–Weiss reactions? Should not there have been a selective advantage to minimize such chaos?

Motivated by these considerations, we hypothesized that the rates of ligand exchange associated with LMPs are actually slow enough for individual metal complexes to be isolated. Perhaps exchange rates have been reduced during evolution by the use of polydentate ligands and donor atoms that afford relatively strong metal–ligand binding interactions.

With the goal of isolating labile metal complexes, we have designed a refrigerated anaerobic liquid chromatography system interfaced with an online inductively coupled plasma mass spectrometer. Our LC–ICP-MS system can split a portion of the eluent to the ICP-MS for detection and send the remainder to a fraction collector. This arrangement allows us to detect, isolate, and eventually characterize the complexes that compose LMPs.

In this study, we have focused on LMPs in mitochondria isolated from fermenting *Saccharomyces cerevisiae* cells. LMPs were assumed to be composed of metal complexes with masses of <10 kDa, rationalized as follows. Most mitochondrial metalloproteins are encoded by nuclear DNA and imported into mitochondria as unfolded polypeptides threaded through the TOM/TIM protein complexes on the outer and inner membranes (OM and IM, respectively).[3] Once in the matrix, a signal sequence is typically clipped, and the apo-metalloprotein folds and is metalated. Metalloproteins encoded by mtDNA are probably metalated by similar mechanisms. In either case, most of the metal ions used in metalation must be transported into the matrix. Because the IM is "tight", these metal ions must enter the matrix through channel-containing IM transport proteins, thereby excluding high-molecular-mass (HMM) species.[4,5] Metal donors must be small enough to pass through pores in the OM, which is limited to masses of less than ~3 kDa.[6] Metalloproteins that localize to the IMS might be metalated by metal complexes that enter the IMS via the OM.[7] However, the Cu ions that metalate IMS metalloproteins have been proposed to pass from the cytosol to the matrix and then to the IMS.[39]

Here we report detection of LMM P, S, Mn, Fe, Co, Cu, Zn, and Mo species, some of which probably function to metalate mitochondrial apo-metalloproteins. We assessed the reproducible occurrence of such species, determined their approximate molecular masses, and estimated their concentrations within the organelle. Our results set the stage for more advanced downstream characterizations.

EXPERIMENTAL PROCEDURES

Strains, Media, and Cell Growth. BY4741 cells (*MATα, ura3Δ0, leu2Δ0, met15Δ0, his3Δ1*) were grown on standard yeast peptone agar plates with 2% glucose (YPD) for 3–4 days. Colonies were inoculated into minimal medium containing 2% (w/v) glucose, 100 mg/L leucine, 50 mg/L adenine hemisulfate dihydrate, 20 mg/L uracil, 20 mg/L histidine, 20 mg/L methionine, and 50 mg/L tryptophan. The endogenous metal ion concentrations of minimal medium were 10 μM Zn, 2 μM Mn, 2 μM Co, 0.3 μM Fe, 0.2 μM Cu, and 5 nM Mo (n = 2). For standard growth, Cu^{II} sulfate and $^{57}Fe^{III}$ citrate were added to the medium to final concentrations of 1 and 10 μM, respectively. In two metal supplementation experiments, 10 μM Cu^{II} sulfate or 100 μM Fe^{III} citrate was added to standard medium. In two other supplementation experiments, 100 μM $Zn(acetate)_2$ or 20 μM $MnCl_2$ (final concentrations) was added. Cells were grown in 24 L batch cultures using a custom-built water-jacketed iron-free glass/titanium bioreactor at 30 °C with O_2 gas bubbled through the medium at a rate of 0.9 L/min. For most batches, cells were harvested in exponential growth phase at an OD_{600} of 0.8 (1 cm path length). Other batches were harvested at an OD_{600} of 1.2–1.6 when cells were undergoing the transition into postexponential growth mode. At the start of each harvest, the bioreactor was set to 5 °C. Human Jurkat cells were grown on 10 μM Fe^{III} citrate as described.[8] C57BL/6 mice were raised and organs dissected as described.[9]

Mitochondrial Isolation and LMM Fractionation. Mitochondria were isolated and manipulated anaerobically in either of two refrigerated (~10 °C) Ar atmosphere glove boxes containing ~5 ppm of O_2. Mitochondria from yeast, human Jurkat cells, and mouse brain and liver tissues were isolated as described.[8,10] Isolated mitochondria were washed two or three times in 50 mM Tris (pH 7.4). For yeast and mammalian mitochondria, 82% and 65% of the packed volume of the isolated organelle were previously determined to be due, respectively, to the mitochondria themselves.[11,12] Assuming these packing efficiencies, pellets were resuspended in 1.0 mL of the same buffer but with 2% Triton X-100. This typically afforded a final volume of 1.4 mL. After being incubated for 15 min while being constantly vortexed, the solution was centrifuged at 12000g for 15 min. The resulting supernatant, called the soluble mitochondrial extract (SME), typically constituted all but ~50 μL of the solution volume. The SME was transferred to an Amicon stirred cell concentrator containing a 10 kDa cutoff membrane, and the flow-through solution (FTS) was collected. Relative to concentrations in intact isolated yeast mitochondria, both SME and FTS were typically 4 times more dilute $[1.4/(0.4 \times 0.82) \approx 4]$.

For each batch, 75 μL aliquots of the SMEs and FTSs were placed in 15 mL nitric acid-rinsed screw-capped polypropylene tubes. Samples were incubated with 100 μL of concentrated trace metal grade nitric acid, sealed with plastic electrical tape, digested for 12 h at 90 °C, and then diluted with water to 10 mL. Resulting solutions were analyzed by ICP-MS. Concentrations were calibrated using primary P, S, Mn, ^{56}Fe, ^{57}Fe, Co, Cu, and Zn standards (Inorganic Ventures, 5000 μg of metal/L each). Secondary standards (0, 10, 50, and 100 μg/L for each metal and 0, 1000, 5000, and 10000 μg/L for P and S) were used for calibration.

LC–ICP-MS experiments were performed in a refrigerated anaerobic glovebox (MBraun Labmaster) at 10 °C and ~5 ppm of O_2. FTSs (500 μL) were injected onto two 10 mm × 300 mm Superdex peptide columns connected in series. The resulting double-length column was equilibrated with 50 mM Tris-HCl (pH 7.4). After injection, the same buffer was

DOI: 10.1021/bi5015437
Biochemistry 2015, 54, 3442–3453

Table 1. Average Concentrations of Selected Elements in Mitochondria[a]

	P (mM)	S (mM)	Mn (μM)	Fe (μM)	Co (nM)	Cu (μM)	Zn (μM)	Mo (μM)
average (HMM+LMM)	28	6.6	16	530	89	71	300	1.4Y;6.3M
standard deviation	3	0.9	3	150	27	34	60	0.4Y;1.2M
10-fold M	–	–	25	780	–	140	480	–
previous average (HMM+LMM)[14−16,51]	–	–	20	630[b]	–	70[c]	280	–
standard deviation	–	–	9	100	–	28	38	–
Ave (LMM)	24	5.4	3.1	116	65	32	140	0.02Y;1M
standard deviation	3	0.6	1.0	32	18	9	21	5Y;0M
10-fold M	–	–	8	170	–	120	280	–
% LMM	86	82	19	22	73	45	47	1.5Y;16M
standard deviation	5	5	6	6	14	20	6	0.9Y;3M

[a]The top group of rows refers to total mitochondrial concentrations. The second group refers to previous reports of metal concentrations in fermenting yeast mitochondria. The third group refers to LMM species only. The bottom group indicates the percent of each selected element that is found in mitochondria as LMM species (based on data from this study). [b]The Fe concentration from ref 15 (1190 μM) was excluded. [c]The Cu concentration from ref 51 (220 μM) was excluded because those cells were grown under respiration conditions where cytochrome *c* oxidase levels are higher. In the Mo column, Y refers to yeast and M to mammalian mitochondria. Numbers in the bottom two rows are given as a percentages, not concentrations.

pumped through the column at a rate of 0.350 mL/min for 166 min using an Agilent Bioinert high-performance liquid chromatography system with titanium pump heads and all-PEEK tubing. The total elution volume (58 mL) corresponded to 2 column volumes (CVs), as determined using Blue Dextran. The eluent passed through a diode array UV−vis detector and into the nebulizer of an Agilent 7700x ICP-MS. The ICP-MS detected ^{31}P, ^{34}S, ^{55}Mn, ^{56}Fe, ^{57}Fe, ^{59}Co, ^{63}Cu, ^{66}Zn, and ^{95}Mo in He collision mode with a dwell time of 0.1 s. After every other run, columns were cleaned with 10 CVs of a chelator cocktail.[13] Elution volumes were calibrated to molecular masses using a series of standards (Figure S1 and Table S1 of the Supporting Information).

The metal concentration corresponding to each peak in the chromatograms was determined as follows. The column was replaced with tubing, and 500 μL of the same elemental standards were injected onto the "phantom column". The resulting "eluent" flowed into the ICP-MS, affording a chromatogram, for each element, composed of a single peak. Each area:concentration ratio was obtained by dividing the integrated areas under the peak by the concentration of the standard injected.

A second method for determining metal concentrations was also used to evaluate the fraction of metal ions that adsorbed onto the column. Areas associated with each peak were determined by fitting. Each peak area was divided by the sum of all areas in the chromatogram. The resulting fractions reflected the proportion of each metal associated with a particular peak. The sum of these areas was assumed to correspond to the total concentration of the metal in the FTS.

If no metals adsorbed onto the column during a run, the concentrations obtained by the second method would equal those obtained by the first. In practice, the two differed by <10%, indicating that the vast majority of the metals in the FTSs eluted from the column.

Five independent batches of mitochondria were isolated from WT yeast cells grown on medium supplemented with 10 μM Fe^{III} citrate and 1 μM $CuSO_4$. The cells were harvested at a low OD_{600} of 0.8 during the exponential phase. Aliquots were subjected to the LC−ICP-MS system immediately (at t = 0) after mitochondria were isolated. To highlight these batch-dependent characteristics (Yeast, Low, t = 0), we will refer to the batches as *YL0A*, *YL0B*, *YL0C*, *YL0D*, and *YL0E* (Table S2 of the Supporting Information). Aliquots of YL0A and YL0B were re-run after being incubated for 5 days in the glovebox; those runs will be called *YL5A* and *YL5B*.

Four other batches were prepared from WT yeast cells grown on the same medium but spiked one at a time with 100 μM Fe, 10 μM Cu, 100 μM Zn, and 20 μM Mn. These batches will be called *YL0Fe*, *YL0Cu*, *YL0Zn*, and *YL0Mn*, respectively. Three other batches were harvested at higher culture densities (postexponential phase), including *YH0A*, *YH0B*, and *YH0C*. An aliquot of YH0B was re-run 5 days after it was initially prepared, generating trace *YH5B*. A batch prepared under respiring (glycerol) conditions will be called *YRL0A*. Three other batches of mitochondria were prepared, including one each from mouse brain, human Jurkat cells, and mouse liver.

RESULTS

Concentrations of selected elements in isolated mitochondria are listed in Table S3 of the Supporting Information; rounded averages are listed in Table 1. Previous studies[14−16] afforded comparable yeast mitochondrial metal concentrations. Concentrations for mammalian mitochondria were similar except for that of Mo, which was ∼4 times higher than in the yeast organelle. Increasing Mn, Fe, Cu, and Zn concentrations 10-fold in the yeast growth medium, one at a time, significantly increased the concentration of that element in isolated mitochondria. The concentrations of the other detected elements, whose concentrations were not increased in the medium, were unaffected. This sensitivity between the medium and mitochondrial metal ion concentrations must be mediated by changes in cytosolic metal ion levels, but the pathways involved are unknown. The absence of secondary perturbations suggests that the homeostatic systems regulating the concentrations of these metals in mitochondria are largely independent of each other.

The concentrations of the LMM forms of these elements in mitochondria are listed in Table S4 of the Supporting Information, with averages again listed in Table 1. No

DOI: 10.1021/bi5015437
Biochemistry 2015, 54, 3442−3453

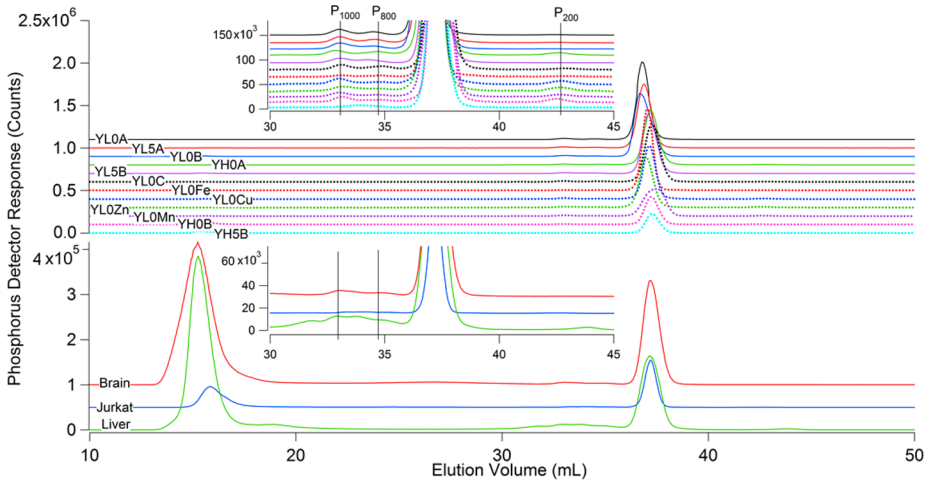

Figure 1. Phosphorus-detected chromatograms of LMM mitochondrial FTSs.

Table 2. LMM Metal Complexes and P and S Compounds in Mitochondria[a]

peak name	center (mL)	width (mL)	molecular mass (Da)	[yeast] (μM)	[mouse] (μM)	[Jurkat] (μM)	R value (%)
P_{1000}	33.4 ± 0.2	0.9 ± 0.1	1000 ± 200	400 ± 100	500	400	100
P_{800}	34.6 ± 0.1	1.3 ± 0.2	800 ± 200	300 ± 100	400	400	100
P_{520}	37.1 ± 0.2	0.7 ± 0.1	520 ± 100	20000 ± 4000	24000	24000	100
P_{200}	42.7 ± 0.2	1.4 ± 0.1	200 ± 50	230 ± 140	100	100	80
S_{1100}	32.8 ± 0.3	1.0 ± 0.1	1100 ± 150	4900 ± 40	6300	6300	100
S_{780}	34.8 ± 0.1	1.4 ± 0.5	780 ± 200	500 ± 400	nd	nd	60
Mn_{2000}	30.5 ± 0.2	1.2 ± 0.1	2000 ± 200	nd	2	3.5	nd
Mn_{1100}	32.6 ± 0.1	0.9 ± 0.1	1100 ± 160	1.9 ± 0.2	2	0.5	100
Fe_{1500}	30.8 ± 0.1	0.8 ± 0.2	1500 ± 300	nd	15	nd	nd
Fe_{1100}	32.7 ± 0.1	1.3 ± 0.2	1100 ± 250	6 ± 2	10	nd	80
Fe_{870}	34.1 ± 0.5	0.7 ± 0.1	870 ± 100	12 ± 9	2	nd	60
Fe_{680}	35.6 ± 0.4	1.1 ± 0.4	680 ± 130	20 ± 10	2	nd	50
Fe_{580}	36.6 ± 0.3	1.4 ± 0.1	575 ± 150	90 ± 20	26	110	100
Fe_{200}	43.3 ± 0.2	1.2 ± 0.8	200 ± 40	2 ± 1	1	nd	90
Co_{1500}	30.8 ± 0.3	0.8 ± 0.2	1500 ± 300	nd	0.01	0.02	90
Co_{1200}	32.3 ± 0.2	0.9 ± 0.1	1200 ± 180	0.03 ± 0.02	0.04	0.04	90
Co_{840}	34.3 ± 0.3	1.7 ± 0.6	840 ± 270	0.02 ± 0.01	0.01	0.02	90
Co_{450}	38.2 ± 0.5	2.4 ± 0.9	450 ± 200	0.013 ± 0.002	nd	nd	70
Co_{340}	39.8 ± 0.2	1.8 ± 0.4	340 ± 100	0.006 ± 0.004	nd	nd	90
Co_{300}	41.1 ± 0.4	2.0 ± 1.5	300 ± 10	0.002 ± 0.001	nd	nd	80
Cu_{5000}	23.1 ± 0.1	1.4 ± 0.2	5000 ± 1000	16 ± 7	nd	nd	90
Zn_{1500}	30.8 ± 0.2	0.7 ± 0.1	1500 ± 200	nd	8	6	nd
Zn_{1200}	32.2 ± 0.2	0.6 ± 0.2	1150 ± 100	110 ± 20	100	100	100
Zn_{900}	34.1 ± 0.1	1.8 ± 1.3	900 ± 300	6 ± 1	nd	nd	100
Mo_{730}	35.0 ± 0.1	0.7 ± 0.1	730 ± 100	nd	0.4	0.3	100

[a]Values were obtained by fitting to Gaussian functions as described in the text.[13] nd means not detected. The R value indicates the confidence in yeast traces only.

significant differences between yeast and mammalian mitochondria were observed except that the average concentration of LMM Mo in mammalian mitochondria was 50 times higher than in yeast. Approximately 80% of P, S, and Co in mitochondria were LMM, while only 20% of Mn and Fe were LMM. Nearly half of the Cu in mitochondria was in the form of LMM complexes. However, some LMM Co and Cu may not be physiologically relevant (see below), lowering these percentage estimates. In mammalian mitochondria, ~16% of Mo in the organelle was present in LMM forms. Nearly half of mitochondrial Zn ions was LMM. Atkinson et al.[17] reported that nearly half of the Zn in sonicated yeast mitochondrial homogenates was soluble; the two results together suggest that most soluble Zn in mitochondria is LMM.

LC–ICP-MS Characterization of FTSs. Mitochondrial FTSs were subjected to anaerobic liquid chromatography. Eluents were monitored for LMM P, S, Mn, Fe, Co, Cu, Zn, and Mo using an online ICP-MS. The abscissas for all chromatograms (Figures 1–7) were adjusted slightly (±0.3 mL) to align two particular phosphorus peaks [Figure 1, P_{1000} and P_{800} (see below)]. Plots of all of the other monitored elements in the same run were adjusted identically (i.e., based on the P alignment).

Concentrations of the reproducibly observed LMM species are listed in Table 2. HMM peaks were often observed at

DOI: 10.1021/bi5015437
Biochemistry 2015, 54, 3442–3453

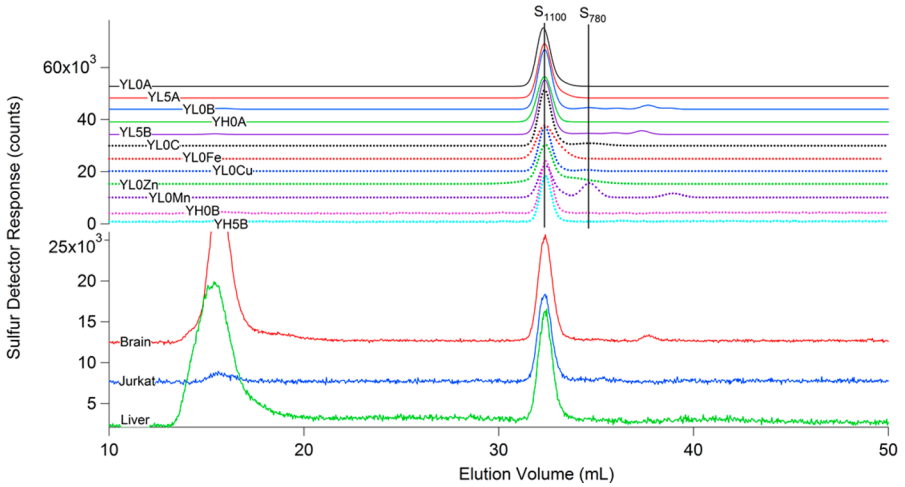

Figure 2. Sulfur chromatograms of LMM mitochondrial FTSs.

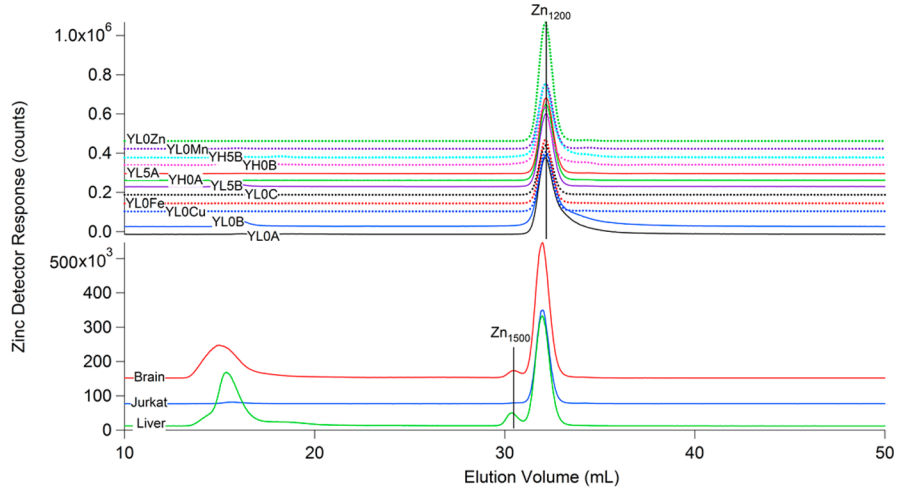

Figure 3. Zinc chromatograms of LMM mitochondrial FTSs.

elution volumes near the void volume (15.3 mL). Such peaks were used in concentration determinations but were not analyzed for molecular mass because the species that migrated in this region were not sufficiently well resolved to allow for accurate molecular mass determinations.

Phosphorus. Yeast mitochondrial FTSs exhibited four major LMM P species with approximate masses of 1000, 800, 520, and 200 Da (Figure 1 and Table 2). We will refer to these as P_{1000}, P_{800}, P_{520}, and P_{200}, respectively. P_{520} exhibited the greatest intensity, followed distantly by P_{1000}, P_{800}, and P_{200}. The concentration of P_{520} in isolated mitochondria was approximately 20 mM. It essentially comigrated with ATP (507 Da). Thus, the majority of the P_{520} peak was assigned to ATP, with ADP (427 Da) thought to contribute to the broadening on the low-mass side of the peak. If this is assumed, the concentration of P_{520} in mitochondria would be ~7 mM (20/3). Yeast mitochondria reportedly contain 7.8 mM ATP.[18] This supports our assignment and adds confidence that our methods of estimating concentrations and masses were reasonably accurate.

P_{1000}, P_{800}, and P_{200} were not assigned. However, the apparent masses of P_{800} and P_{200} were similar to those of NADPH (744 Da) and pyrophosphate (174 Da). If these assignments were correct, the concentrations of these species in mitochondria would be 100 and 200 μM, respectively. Reported concentrations of NADPH in mitochondria and cytosol range between 45 and 235 μM,[19] which are in the same ballpark.

The P content of mammalian mitochondria was similar to that of yeast; P_{520} again dominated, and the same minor-intensity species were evident. In the P chromatogram of mitochondria from Jurkat cells, the same minor-intensity peaks were present, but their intensities were lower than in the other mammalian samples. The chromatograms of liver and brain mitochondrial FTSs exhibited additional P-containing species that were not assigned.

Sulfur. Mitochondrial FTSs consisted of two major S peaks, corresponding to masses of 1100 and 780 Da (Figure 2 and Table 2). S_{1100} dominated and was reproducibly present at concentrations near 5 mM. The presence of S_{780} was more sporadic. Surprisingly, neither species comigrated with glutathione (GSH, 307 Da) or glutathione disulfide (GSSG, 612 Da); further studies are needed to explain this given the abundance of glutathione in mitochondria. Authentic GSSG migrated in accordance with its mass, including in a run of FTS spiked with GSSG. Authentic GSH appears to oxidize as it migrates through the column, but the details of this are under investigation.

DOI: 10.1021/bi5015437
Biochemistry 2015, 54, 3442−3453

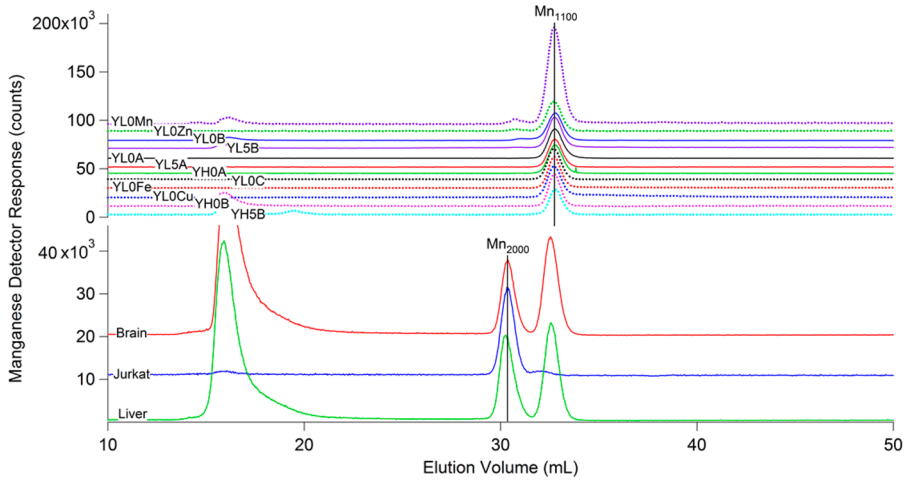

Figure 4. Manganese chromatograms of LMM mitochondrial FTSs.

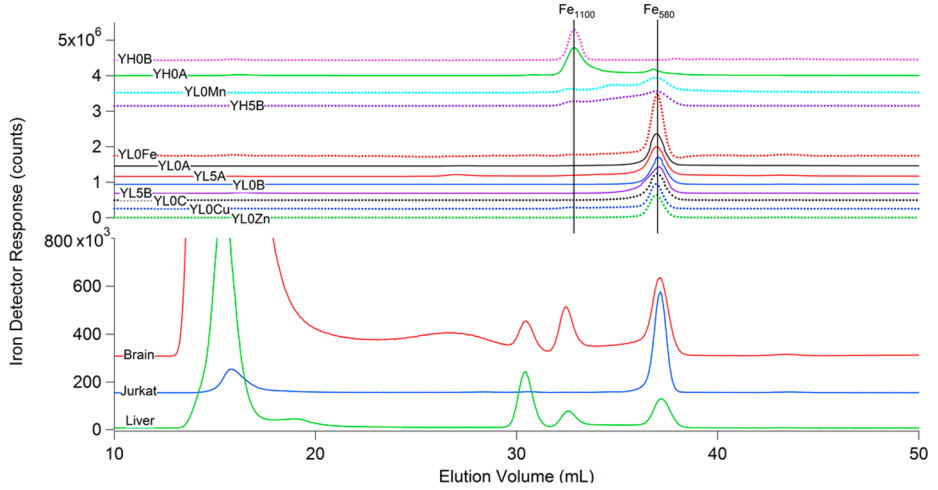

Figure 5. Iron chromatograms of LMM mitochondrial FTSs.

Zinc. Yeast mitochondrial FTSs exhibited an intense Zn peak corresponding to a mass of 1200 Da (Figure 3 and Table 2). The concentration of Zn_{1200} in yeast mitochondria was 110 μM, nearly half of the total Zn in the organelle and almost all of the soluble Zn. The same species was in FTSs from mammalian mitochondria. A minor-intensity species with a mass of ~900 Da (Zn_{900}) was in yeast mitochondria at a concentration of ~1 μM. Mitochondria from yeast grown on medium containing 10-fold more Zn than normal exhibited a 2.5-fold increase in the intensity of Zn_{1200}, whereas the intensities for the other peaks were not significantly affected. A higher-mass species (Zn_{1500}) was detected in mitochondria from brain and liver but not yeast.

Manganese. A single LMM Mn species with a mass of 1100 Da (Mn_{1100}) dominated the chromatograms of fermenting yeast mitochondrial FTSs (Figure 4 and Table 2). A minority species of higher mass (Mn_{2000}) was in some FTSs. The concentration of Mn_{1100} in yeast mitochondria was ~2 μM, while that of Mn_{2000} was 23-fold lower. The Mn_{1100} concentration increased 4-fold in mitochondrial FTS from yeast cells grown in media containing 10-fold normal Mn; the concentration of Mn_{2000} also increased, albeit more modestly.

Both Mn_{2000} and Mn_{1100} were in mitochondrial FTSs from human cells and mouse tissues, but the relative intensities differed significantly from those in yeast. In mitochondria from Jurkat cells, Mn_{2000} represented ~95% of the Mn in the organelle, with minor contributions from Mn_{1100}. The concentrations of these two species in mitochondria from mouse brain and liver were more balanced, affording concentrations of 1−2 μM each. We previously observed a single LMM Mn species in yeast mitochondria with a mass between 2000 and 3000 Da.[20] Such a species was not observed currently in fermenting yeast mitochondria but was observed in our one batch of respiring yeast mitochondria (YRL01). A systematic study is required, but we currently suspect metabolism-dependent effects.

Iron. Yeast mitochondrial FTSs exhibited two major Fe species (Fe_{580} and Fe_{1100}), with either species dominating depending on (a) the mode of growth of the cells at the time of harvesting and (b) whether the FTS was chromatographed immediately after it was prepared or 5 days later. Mitochondrial FTSs isolated from cells harvested during exponential growth and run immediately exhibited Fe_{580} (Figure 5 and Table 2). A low-intensity peak corresponding to a higher-mass species (Fe_{1100}) was also evident. The chromatogram from mitochondrial FTS obtained from cells grown on medium containing 100 μM Fe^{III} citrate (rather than the standard 10 μM) exhibited a 1.7-fold increase in the intensity of the Fe_{580} peak.

Fe-detected chromatograms of FTSs isolated from cells harvested during the postexponential growth phase and run

DOI: 10.1021/bi5015437
Biochemistry 2015, 54, 3442−3453

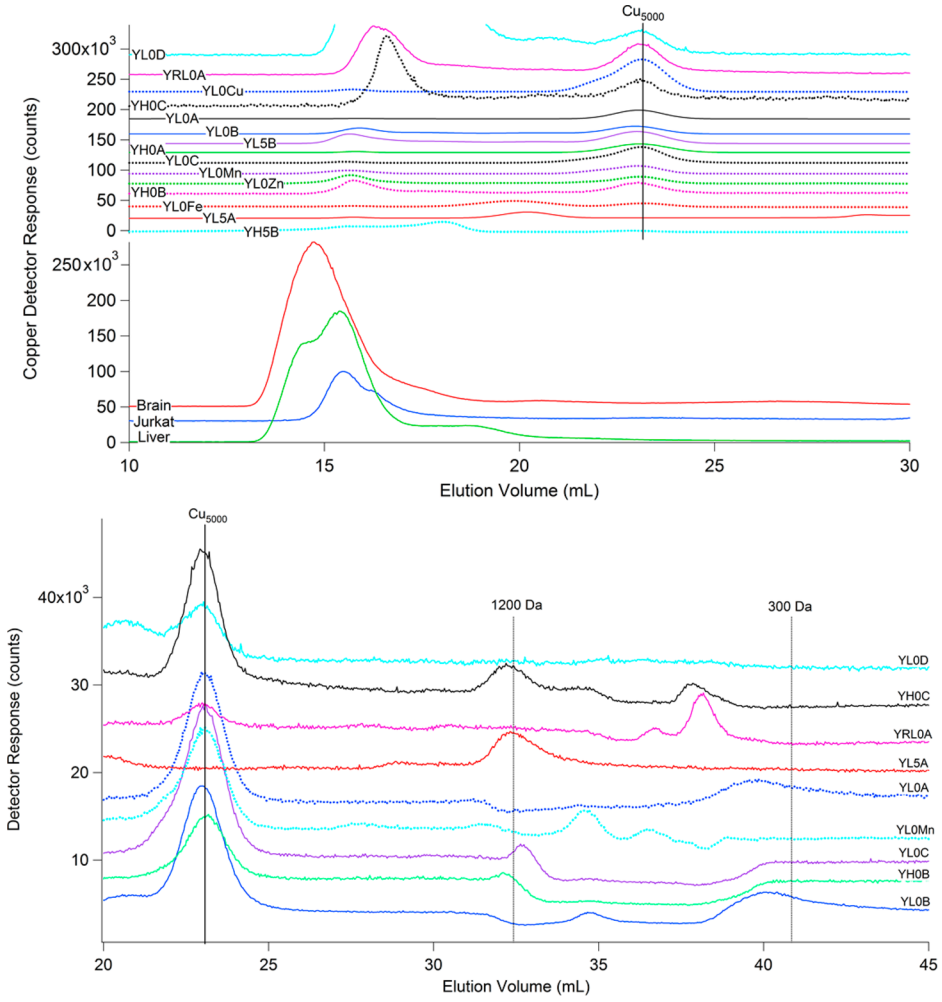

Figure 6. Copper chromatograms of LMM mitochondrial FTSs.

immediately after isolation were dominated by Fe_{1100}. Fe_{580} was present but at a reduced intensity. Unexpectedly, when a FTS dominated by Fe_{1100} was left in a refrigerated glovebox for 5 days, the resulting chromatogram was dominated by Fe_{580}, with Fe_{1100} downgraded to a minor component. In that chromatogram, another Fe-containing species with an intermediate mass was also evident. For reasons that we do not understand, trace YL0Mn exhibited a more highly resolved species with a mass of 870 Da (Fe_{870}) (Figure 5). During incubation, Fe_{1100} may convert into Fe_{580} via intermediate Fe_{870}. The only other Fe species present exhibited a very low intensity peak associated with a mass of 200 Da. Because hexaqua Fe has a mass of ~160 Da, we assign Fe_{200} as such. The concentration of Fe_{200} in our isolated mitochondria samples was 1−3 μM, which we regard as an upper limit of what it might be in intact mitochondria (one-half of 1% of the Fe in mitochondria). Fe_{200} may be an artifact of the isolation procedure, with healthy mitochondria devoid of this species.

Iron chromatograms of FTSs from mitochondria isolated from mammalian cells and tissues were similar to those of yeast, but with additional peaks. The chromatogram of FTS from mitochondria of Jurkat cells was similar to that of yeast harvested during the exponential growth phase, with Fe_{580} dominating. The chromatogram from mouse tissues also exhibited Fe_{580}, but intense peaks corresponding to masses of 2000 and 1200 Da (Fe_{2000} and Fe_{1200}, respectively) were also observed. Fe_{2000} was not present in yeast mitochondria. Fe_{1200} in mouse mitochondria may or may not correspond to Fe_{1100} in yeast mitochondria; the two migrated near each other, but they did not comigrate. Concentrations of Fe_{2000} and Fe_{1100}/Fe_{1200} in mammalian mitochondria were ~10 μM each.

Copper. FTSs from mammalian mitochondria exhibited Cu peaks near or slightly beyond the 10 kDa cutoff (Figure 6, top panel). The observed intensities of Cu species with masses of >10 kDa may be less than proportional to their actual concentration in mitochondria, as some of these species may have been retained by the cutoff membrane. These cutoffs are not exact, such that some proportion of higher-mass Cu species also passes into the FTS, as observed. Also, our size-exclusion column has some resolving power beyond 10 kDa. For example, cytochrome *c* (Table S1 of the Supporting Information, 12384 Da) fell nicely on the calibration line (Figure S1 of the Supporting Information), although its mass is beyond the formal resolving limit of the column. Thus, a Cu complex with a mass of ~13 kDa would be detected and resolved by our experiment; indeed, such features are observed in FTSs from mammalian mitochondria.

The region between 10000 and 2000 Da exhibited the greatest reproducibility (Figure 6, top panel). Cu-detected chromatograms of the FTS of mitochondria from yeast cells were dominated by a peak corresponding to a mass of 5000 Da; the corresponding concentration was ~16 μM. Cu_{5000}

DOI: 10.1021/bi5015437
Biochemistry 2015, 54, 3442−3453

accounted for ~60% of the Cu in the FTS and ~20% of Cu in yeast mitochondria. With a mass of 5000 Da, Cu_{5000} might be proteinaceous. The intensity of this species increased 4-fold when the Cu concentration in the medium was increased 10-fold. Curiously, the Cu-detected chromatograms of the mammalian system did not exhibit Cu_{5000} or any other peak in 2000−10000 Da region. This was similar to the results of our previous study of mouse brain LMM extracts, in which no LMM Cu species were reproducibly evident but many HMM Cu species (8−48 kDa) were observed.[13]

For mitochondrial FTSs, the region between 200 and 2000 Da exhibited minor-intensity peaks with significant preparation-to-preparation variation (Figure 6, bottom panel). At the high sensitivity required to observe these peaks, some baseline drift is evident. Peaks corresponding to masses of ~300 Da may reflect hydrated Cu ions. The poorer reproducibility and low-intensity character of these LMM Cu-based peaks suggest that some Cu ions may dissociate from their endogenous complexes during mitochondrial isolation, and that the released ions coordinate to various ligands.

Cobalt. The Co-detected chromatograms of mitochondrial FTSs exhibited many peaks between 1200 and 300 Da (Figure 7 and Table 2), albeit with more batch-to-batch variability than

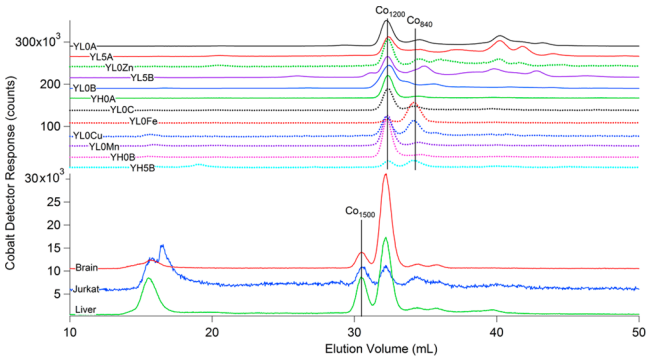

Figure 7. Cobalt chromatograms of LMM mitochondrial FTSs.

for most other metals. The concentration of the dominant peak at 1200 Da (Co_{1200}) was 30 nM, 3 orders of magnitude lower than for many other LMM metal species. The similar masses of various cobalamins (1300−1700 Da) suggest that Co_{1200} is a cobalamin. FTS from yeast mitochondria exhibited other Co peaks, corresponding to masses between 840 and 200 Da, but the batch-to-batch variation in the intensity of these peaks was significant. Peaks in the 200 Da region were probably hydrated Co ions. Peaks corresponding to masses between 300 and 800 Da were probably not cobalamins as their masses were too low; their concentrations were in the nanomolar range.

Co chromatograms of mammalian samples were similar to each other, except that the intensities of the Co peaks in the Jurkat sample were very low. FTSs of mammalian mitochondria contained Co_{1200} as well as another cobalamin (Co_{1700}) with a mass of 1700 Da.

Molybdenum. Chromatograms of mammalian mitochondria FTSs exhibited a single Mo peak (Mo_{730}) at 730 Da (Figure S2 of the Supporting Information and Table 2). No Mo species were detected in fermenting yeast mitochondrial FTSs.

Lability of LMM Metal Complexes. We assessed whether 1,10-phenanthroline (phen) and bathophenanthroline disulfonate (BPS) could chelate the metal ions in the detected complexes. The FTS from a batch of yeast mitochondria was subjected to the LC−ICP-MS system, and Fe, Zn, Co, Mn, and Cu chromatograms were obtained (Figure S3 of the Supporting Information, black lines). Fractions containing LMM metal complexes were pooled and treated with BPS, but this had little effect. After being treated with BPS, phen, and the reductant dithionite, the same pool exhibited chromatograms whose peaks were significantly changed (Figure S3 of the Supporting Information, red lines). The changes were numerous and dramatic, such that further systematic studies are required to interpret them. It is clear, however, that the dominant LMM metal complexes in yeast mitochondria can be labilized by metal chelators.

DISCUSSION

In this study, we detected numerous LMM P, S, Mn, Fe, Co, Cu, and Zn compounds in mitochondria isolated from yeast and mammalian cells. A LMM Mo complex was detected exclusively in mitochondria from mammalian cells. We cataloged each and estimated their molecular mass and concentration within the organelle. The model of Figure 8

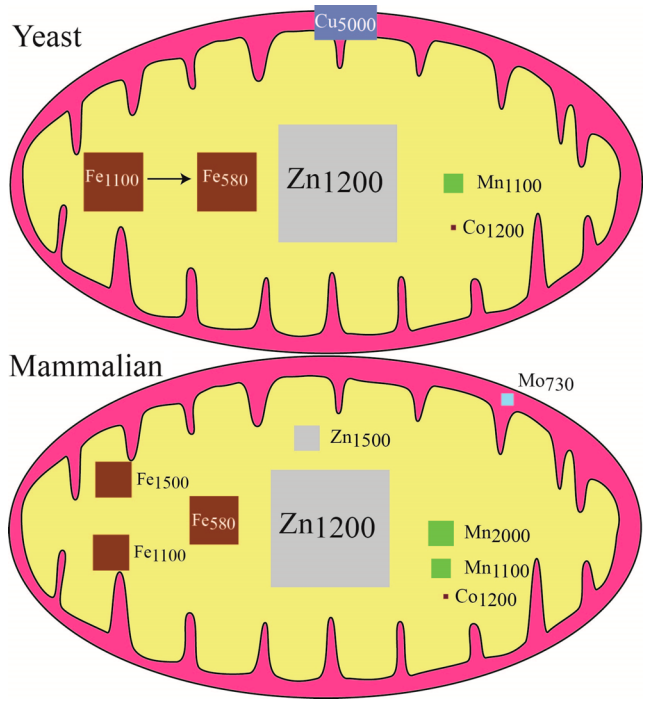

Figure 8. Model of LMM metal complex speciation in yeast and mammalian mitochondria. The sizes of the colored squares represent the relative concentrations of various LMM species. Other details are given in the text.

illustrates the major detected species, including concentrations and suggested locations in the organelle. Most of these metal complexes are presumed to be in the matrix and used to metalate apo-metalloproteins. Cu_{5000} in yeast mitochondria and Mo_{730} in mammalian mitochondria may be located in the IMS. Further studies are required to establish their locations, compositions, structures, and biochemical and physiological functions.

We previously detected a single Mn species in yeast mitochondria and proposed that it metalated apo-SOD2.[20] We now assign this role to Mn_{1100} despite a slightly lower mass. Mammalian mitochondria contain a second Mn enzyme, Type

DOI: 10.1021/bi5015437
Biochemistry 2015, 54, 3442−3453

II arginase,[21,22] that catalyzes the synthesis of ornithine and may regulate the production of NO by nitric oxide synthase. An enzyme precursor is imported into the matrix where a signal sequence is clipped, and the protein folds and is metalated, perhaps by a second Mn complex in these organelles, Mn_{2000}.

Zn_{1200} in yeast mitochondria and Zn_{1200}, Zn_{900}, and Zn_{1500} in mammalian mitochondria probably compose the labile Zn pool that metallates various mitochondrial Zn proteins.[17] High concentrations of mitochondrial Zn inhibit respiration.[23,24] Perhaps ferrochelatase installs Zn_{1200} rather than Fe^{II} into protoporphyrin IX.[25] Mitochondria from neuronal cells contain Zn that can be mobilized and released when the IM is depolarized.[26] Mobilized Zn ions may correspond to one or more detected LMM Zn species.

Using fluorescence resonance energy transfer-based sensors, Palmer and co-workers detected labile Zn in mitochondria of HeLa cells.[27] McCranor et al.[28] used human carbonic anhydrase II variants to detect labile Zn in rat mitochondria. Labile Zn was detected in mitochondria from mammalian cells using modified GFP fused to calmodulin.[26,29] Chyan et al.[30] used a synthetic fluorescent probe to detect labile Zn in prostate cells. When the medium was spiked with 50 μM Zn, the fluorescence intensity of the mitochondria in normal cells increased 2.3-fold.

We anticipated that the Zn species detected in our study would be the same as those detected by fluorescence-based methods. However, if the reported concentration of the fluorescence-detected Zn species is accurate, we have not detected them. McCranor et al.[28] concluded that the concentration of labile Zn in mitochondria isolated from a rat cell line was 0.15 pM. Virtually the same concentration was reported for the labile Zn pool in mitochondria of HeLa cells.[27] These concentrations are 1 billion times lower than our estimates for the concentration of Zn_{1200}. Our LC−ICP-MS system simply cannot detect picomolar concentrations (1 pM Zn = 0.07 ppt), so our ability to detect Zn species implies that they are present at concentrations greater than hundreds of picomolar.

Another consideration is that the collective volume of mitochondria in cells is just a few percent of the volume of a yeast cell, suggesting a mitochondrial volume of $\sim 10^{-15}$ L. Within this volume, a concentration of 0.15 pM would correspond to 10^{-4} molecules of labile mitochondrial Zn per cell. This implies that just 1 of every 10000 cells would contain mitochondria with a single labile Zn ion, a property that should be easily distinguished from that in which all mitochondria in a cell population uniformly fluoresce when treated with a sensor. As far as we are aware, there have been no reports of stochastic single-molecule fluorescence in these organelles. This implies that each mitochondrion contains a sizable number of labile Zn ions, which implies, in turn, a labile Zn concentration orders of magnitude higher than reported.

In contrast, our Zn results are fully consistent with those of Atkinson et al.,[17] who used LC to detect a LMM cationic Zn pool in the matrix of yeast mitochondria. Their reported pool probably corresponds to Zn_{1200}. The Zn ions in their pool migrate through a Sephadex G25 column in accordance with a mass slightly lower than that of vitamin B_{12} (1355 Da), within error of the mass of our Zn_{1200}. The size of their Zn pool increases when the growth medium is supplemented with Zn, similar to what we observed with Zn_{1200}. The Zn species composing their pool is cationic (implying ligands that on average are uncharged), resistant to boiling, and inert toward proteinase K digestion (implying that it is nonproteinaceous). This species was proposed to metalate numerous Zn enzymes in the matrix, including alcohol dehydrogenases, Leu9, and cytochrome *c* oxidase. Depleting this pool (by placing the apo form of a Zn enzyme into the matrix) causes a respiratory growth defect, consistent with Zn_{1200} serving to metalate proteins required for respiration.

Lutz et al.[31] discovered that 1,10-phenanthroline inhibits Fe/S cluster assembly in intact mitochondria. Similar results were obtained by Amutha et al.[32] and Pandey et al.,[33] who speculated that mitochondria must contain a pool of Fe that is used as feedstock for Fe/S cluster assembly. Phen was thought to penetrate the matrix and coordinate the pool, making it unavailable for Fe/S cluster assembly. Unaware of those results, Holmes-Hampton et al.[34] performed the same experiment in which phen was added to intact ^{57}Fe-enriched mitochondria. Using Mössbauer spectroscopy, they discovered a pool of non-heme high-spin (NHHS) Fe^{II} ions that were selectively chelated by phen. When considered with the results of Lutz, Amutha, and Pandey, the pool of NHHS Fe^{II} ions very likely functions as feedstock for Fe/S cluster biosynthesis. The associated Mössbauer parameters indicate an Fe^{II} species with five or six oxygen and nitrogen donors but no sulfurs. This HS $Fe^{II}(O/N)_{5-6}$ species appears to be in equilibrium with a HS Fe^{III} species and with Fe^{III} oxyhydroxide nanoparticles.[14,34] The concentration of NHHS Fe^{II} that constitutes this pool depends on the metabolic state of the cells from which the mitochondria are isolated. In fermenting mitochondria, the concentration of the NHHS Fe^{II} was $\sim$150 μM, whereas in respiring mitochondria, it was much lower. Because the concentrations of respiratory complexes are 3 times higher in respiring mitochondria, Morales et al.[14] proposed that this decline was due to an increased rate of Fe/S cluster assembly (and an invariant rate of import of Fe into the pool) under respiration conditions.

Rauen et al.[35] detected a labile Fe pool in mitochondria using rhodamine-based fluorescence sensors and estimated a concentration of $\sim$16 μM.[36] It is intriguing to consider that the same species detected by fluorescence is the NHHS Fe^{II} species detected by Mössbauer spectroscopy and used for Fe/S cluster assembly. The 10-fold disparity in concentration may reflect differences in the cells used or different metabolic conditions.

In this study, we have detected two LMM Fe complexes in mitochondria, Fe_{1100} and Fe_{580}. This contrasts with our previous results in which a single LMM Fe complex with a mass of $\sim$3000 Da was detected in soluble extracts of mitochondria isolated[20] from fermenting yeast cells harvested as they entered postexponential growth. There may have been a systematic error in calibrating masses, but we cannot identify any. More likely, different Fe species may be present, depending on metabolic conditions or preparation methods.

The collective concentration of Fe_{1100} and Fe_{580} in mitochondria was $\sim$100 μM; some chromatograms were dominated by one Fe species, while others were dominated by the other. Fe_{1100} and Fe_{580} appear to be related, as the former transformed into the latter by simple incubation of the FTS for 5 days in a refrigerated inert atmosphere. Although much remains to be learned regarding this relationship and the function of these species, we tentatively suggest the following model:

DOI: 10.1021/bi5015437
Biochemistry 2015, 54, 3442−3453

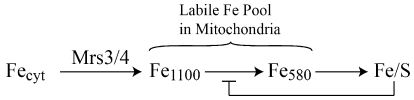

The key feature of this relationship is that the level of Fe/S clusters in the matrix inhibits the conversion of Fe_{1100} to Fe_{580}. During exponential growth, the steady-state level of Fe/S clusters is low because the clusters are quickly being installed into various apoprotein targets. This relieves the inhibition, such that Fe_{1100} levels decline and Fe_{580} levels rise (as observed). As cell growth declines, the steady-state level of Fe/S clusters builds, which strengthens the inhibition of the transforming reaction. Thus, Fe_{1100} accumulates, and Fe_{580} declines (again as observed). This model must be tested further; it currently serves merely to organize our results. The role of Fe_{1500} in mammalian cells remains unknown.

Curiously, the dominant S, Mn, Zn, and Fe (at high culture density) species in fermenting yeast mitochondria all have molecular masses of ∼1100−1200 Da. One interesting possibility is that all of these complexes possess a similar coordination environment that includes sulfur as a ligand. Metal glutathione complexes have been proposed as trafficking ligands in eukaryotic cells.[37−39] Conceivably, these metal complexes might be related to $[M(SG)_4]^{2-}$, which would have a mass of ∼1300 Da. Further studies are required to evaluate this possibility.

Winge and Cobine reported that 70−85% of the Cu in mitochondria is a nonproteinaceous species that serves trafficking and/or metallating functions.[40−42] They considered this species (Cu_L) to be "low-molecular weight", but it migrates in accordance with a 13 kDa globular protein.[40] The complex with characteristics most like those of Cu_L is Cu_{5000}. Like that of Cu_{5000}, the concentration of Cu_L is sensitive to the concentration of Cu in the medium; the level of Cu_L increases 6-fold in cells grown in medium supplemented with 500 μM Cu.[40,41] One difference is that Cu_L is found in both yeast and mouse liver mitochondria, while we have detected Cu_{5000} in only yeast mitochondria. More of the Cu ions in mammalian mitochondria are in a HMM form, including some Cu species with masses near 13 kDa.

Cu_{5000} accounted for 22% of the Cu in mitochondria (16 μM of 71 μM total). Morales et al.[14] estimated that the concentration of cytochrome *c* oxidase in fermenting yeast mitochondria was ∼8 μM, implying ∼24 μM Cu (there are three Cu ions per enzyme molecule). Combining these two concentrations (16 + 24 = 40 μM) leaves ∼30 μM for all other Cu-binding proteins in mitochondria, including Sco1/2, Cox17, CuZn SOD1, CCS1, and Cu_L. Cu_L has been estimated to represent 85% of the Cu in yeast mitochondria.[43] In our preparations, this would correspond to 60 μM. The region between 2000 and 200 Da was devoid of any peak with an intensity corresponding to anywhere near 60 μM (observed peaks are roughly 1/100th of this concentration).

Many studies have detected labile Cu in mitochondria, all of which have been attributed to Cu_L. Dodani et al.[44] developed a fluorescent sensor (Mito-CS1) that selectively targets the mitochondria of HEK293T cells and human fibroblasts where it binds a labile Cu^I species. Yang et al.[45] used a custom-designed fluorescent sensor along with synchrotron X-ray fluorescence to detect labile Cu in mitochondria. Their data indicate a Cu^I complex with linear or trigonal geometry and primarily sulfur coordination.

Our experiment with phen suggests that Cu_{5000} is labile, raising the possibility that the fluorescence-detected labile Cu in mitochondria might arise from Cu_{5000} rather than (or in addition to) Cu_L. However, the absence of Cu_{5000} or other LMM Cu species in mitochondria from mammalian cells would seem to argue against this possibility. Also uncertain is the question of whether Cu_{5000} (or Cu_L or some other Cu-trafficking species) is used to metalate cytochrome *c* oxidase. Cu is thought to be imported into the matrix via Pic2, a mitochondrial carrier family protein.[46] Cu_L in the matrix has also been suggested to metalate the Cu-containing proteins in the IMS,[47] but further studies are required to establish this. Given the size of Cu_{5000}, transporting it across the IM from the matrix to the IMS seems unlikely. The possibility that the Cu used to metalate cytochrome *c* oxidase travels from the cytosol directly to the IMS should be reconsidered. Cu_{5000} may be just small enough to pass through the pores of the OM. However, further studies are needed to evaluate these ideas.

The concentrations of LMM Co species observed here were very low, leading us to wonder whether they are physiological. They may correspond to cobalamin degradation products, possibly including hydrated Co ions at ∼200 Da. Cobalamins are noncovalently attached to proteins, and tiny quantities may have been released during isolation. Alternatively, the observed species may be trafficking complexes that metalate methylmalonyl-CoA mutase, the only known cobalamin-containing mitochondrial enzyme.[48] Cobalamins are not synthesized by mammalian cells but are imported as vitamin B_{12}. The mechanism by which B_{12} enters mitochondria involves trafficking proteins CblB, CblC, and CblD.[48]

The presence of a LMM Mo species (Mo_{730}) in mammalian mitochondria and its absence in yeast mitochondria are consistent with the presence of mitochondrial amidoxime reducing components 1 and 2 (mARC1/2) in mammalian mitochondria and the absence of these and any other Mo-containing enzymes in yeast. mARC1/2 are molybdopterin-containing proteins found in the OM of mitochondria,[49] where they catalyze the reduction of NO_2^- to NO and might be involved in a signaling pathway that regulates NADH-dependent hypoxic NO production.[50] The mass of Mo_{730} is within the range of molybdopterins (albeit with two pterin coenzymes coordinated). Mo_{730} may be associated with the metalation of mARC1/2. Alternatively, it may reflect a tiny amount of a molybdopterin released into solution during mitochondrial isolation.

We have used the same LC−ICP-MS system to detect LMM metal complexes in mouse brain homogenates, including complexes found in mitochondria and other regions of the brain.[13] At this early stage of investigation, we have focused solely on identifying common species. We suggest the following correspondences: P_{490}(brain) ≈ P_{520}(mito), S_{940}(brain) ≈ S_{1100}(mito), Fe_{1720}(brain) ≈ Fe_{1500}(mito), Fe_{510}(brain) ≈ Fe_{580}(mito), Zn_{1760}(brain) ≈ Zn_{1500}(mito), Mn_{2710}(brain) ≈ Mn_{2000}(mito), and Mn_{1270}(brain) ≈ Mn_{1100}(mito). More work is needed to establish these associations.

The regulatory mechanisms used to sense the concentrations of these metals in the environment and to control the corresponding concentrations in the cytosol and mitochondria are not understood. The increased concentrations of particular LMM metal complexes when cells were grown on media that contained higher-than-normal concentrations of the same metal ion undoubtedly reflect such mechanisms. We suspect that (a) the rate of import of metal into the cytosol increases with the increase in nutrient metal concentration and (b) the increased cytosolic metal concentration increases the rate of import of

DOI: 10.1021/bi5015437
Biochemistry 2015, 54, 3442−3453

metal from the cytosol into the mitochondria. Systematic studies are required to probe the specific nature of this regulation.

In summary, we have detected numerous labile LMM metal complexes in mitochondria using an LC−ICP-MS approach. The major advantage of this approach, relative to the more popular fluorescence-based metal binding probes, is that a portion of the detected metal complexes need not be destroyed. Keeping the complexes intact will allow for further downstream characterizations. The LC−ICP-MS method also allows individual metal complexes to be separated and cataloged such that the vague "pool" concept can eventually be discontinued. Also, the area under each chromatography peak can be quantified, thereby allowing estimates of the metal complex concentrations within cells and organelles.

The LC−ICP-MS approach does suffer some disadvantages, the most important being that cells must be disrupted during the preparation of extracts. Doing so could mix cellular compartments, altering the pH and redox state of the environment in which the metal complexes exist. This might, in turn, induce ligand exchange or other reactions, resulting in artifacts that could easily be mistaken for bona fide endogenous metal complexes. Indeed, some metal complexes that we have detected here might be artifacts. Both the LC−ICP-MS approach and the fluorescence-based chelator approach will ultimately be required to detect, catalog, identify, and characterize the structure and function of these recalcitrant cellular components. Doing so will afford a far more sophisticated view of transition metal ion trafficking and regulation in cells, which should, in turn, provide significant new insights into metal-associated diseases.

■ ASSOCIATED CONTENT

Supporting Information

Calibration curve for determining molecular masses based on the migration through the size-exclusion column (Figure S1), compounds used for calibrating the size-exclusion columns (Table S1), nomenclature of LC batches (Table S2), concentrations of selected elements in isolated mitochondria (Table S3), concentrations of selected elements present as LMM species in isolated mitochondria (Table S4), molybdenum chromatograms of FTS (Figure S2), and lability of LMM metal complexes (Figure S3). The Supporting Information is available free of charge on the ACS Publications website at DOI: 10.1021/bi5015437.

■ AUTHOR INFORMATION

Corresponding Author

*E-mail: Lindahl@chem.tamu.edu. Phone: (979) 845-0956. Fax: (979) 845-4719.

Author Contributions

S.P.M. designed and operated the LC−ICP-MS system, analyzed the data, and prepared the figures. M.J.M. grew cells, isolated mitochondria, and prepared samples. P.A.L. offered advice and wrote much of the paper. All authors designed the experimental approach, edited the paper, and approved the final version. S.P.M. and M.J.M. contributed equally to this work.

Funding

This study was funded by the National Institutes of Health (GM084266) and the Robert A. Welch Foundation (A1170).

Notes

The authors declare no competing financial interest.

■ ABBREVIATIONS

FTS (or FTSs), flow-through solution (or solutions); HMM, high-molecular-mass; ICP-MS, inductively coupled plasma mass spectrometry (or spectrometer); LC, liquid chromatography; LC−ICP-MS, a system consisting of an LC in a refrigerated argon atmosphere glovebox interfaced online to an ICP-MS; LMM, low-molecular-mass; OD_{600}, optical density at 600 nm; SME, soluble mitochondrial extract; YL0A, YL0B, YL0C, YL0D, and YL0E, five independent LC experiments using mitochondria from yeast cells that were harvested at a low OD_{600} and applied immediately (t = 0) to the LC column; YL0Fe, YL0Cu, YL0Zn, and YL0Mn, same as above but with the growth medium supplemented with 10-fold normal levels of Fe, Cu, Zn, and Mn, respectively; YH0A, YH0B, and YH0C, three independent LC experiments using mitochondria from yeast harvested at a high OD_{600} and applied immediately to the column; YL5A, YL5B, and YH5B, three LC experiments in which samples were applied to the LC column 5 days after YL0A, YL0B, and YH0B, respectively, were prepared; YRL0A, batch prepared under respiring (glycerol) conditions.

■ REFERENCES

(1) Breuer, W., Shvartsman, M., and Cabantchik, Z. I. (2008) Intracellular labile iron. *Int. J. Biochem. Cell Biol. 40*, 350−354.

(2) New, E. J. (2013) Tools to study distinct metal pools in biology. *Dalton Trans. 42*, 3210−3219.

(3) Dudek, J., Rehling, P., and van der Laan, M. (2013) Mitochondrial protein import: Common principles and physiological networks. *Biochim. Biophys. Acta 1833*, 274−285.

(4) Atkinson, A., and Winge, D. R. (2009) Metal Acquisition and Availability in the Mitochondria. *Chem. Rev. 109*, 4708−4721.

(5) Pierrel, F., Cobine, P. A., and Winge, D. R. (2007) Metal Ion availability in mitochondria. *BioMetals 20*, 675−682.

(6) Benz, R. (1990) Biophysical Properties of Porin Pores from Mitochondrial Outer-Membrane of Eukaryotic Cells. *Experientia 46*, 131−137.

(7) Terziyska, N., Lutz, T., Kozany, C., Mokranjac, D., Mesecke, N., Neupert, W., Herrmann, J. M., and Hell, K. (2005) Mia40, a novel factor for protein import into the intermembrane space of mitochondria is able to bind metal ions. *FEBS Lett. 579*, 179−184.

(8) Jhurry, N. D., Chakrabarti, M., McCormick, S. P., Gohil, V. M., and Lindahl, P. A. (2013) Mössbauer study and modeling of iron import and trafficking in human jurkat cells. *Biochemistry 52*, 7926−7942.

(9) Holmes-Hampton, G. P., Chakrabarti, M., Cockrell, A. L., McCormick, S. P., Abbott, L. C., Lindahl, L. S., and Lindahl, P. A. (2012) Changing iron content of the mouse brain during development. *Metallomics 4*, 761−770.

(10) Chakrabarti, M., Cockrell, A. L., Park, J., McCormick, S. P., Lindahl, L. S., and Lindahl, P. A. (2015) Speciation of iron in mouse liver during development, iron deficiency, IRP2 and inflammatory hepatitis. *Metallomics 7*, 93−101.

(11) Lindahl, P. A., Morales, J. G., Miao, R., and Holmes-Hampton, G. (2009) Isolation of *Saccharomyces cerevisiae* mitochondria for Mössbauer, EPR, and electronic absorption spectroscopic analyses. *Methods Enzymol. 456*, 267−285.

(12) Jhurry, N. D., Chakrabarti, M., McCormick, S. P., Holmes-Hampton, G. P., and Lindahl, P. A. (2012) Biophysical investigation of the ironome of human Jurkat cells and mitochondria. *Biochemistry 51*, 5276−5284.

(13) McCormick, S. P., Chakrabarti, M., Cockrell, A. L., Park, J., Lindahl, L. S., and Lindahl, P. A. (2013) Low-molecular-mass metal complexes in the mouse brain. *Metallomics 5*, 232−241.

DOI: 10.1021/bi5015437
Biochemistry 2015, 54, 3442−3453

(14) Morales, J. G., Holmes-Hampton, G. P., Miao, R., Guo, Y. S., Münck, E., and Lindahl, P. A. (2010) Biophysical characterization of iron in mitochondria isolated from respiring and fermenting yeast. *Biochemistry 49*, 5436−5444.
(15) Miao, R., Martinho, M., Morales, J. G., Kim, H., Ellis, E. A., Lill, R., Hendrich, M. P., Münck, E., and Lindahl, P. A. (2008) EPR and Mössbauer spectroscopy of intact mitochondria isolated from Yah1p-depleted *Saccharomyces cerevisiae*. *Biochemistry 47*, 9888−9899.
(16) Holmes-Hampton, G. P., Jhurry, N. D., McCormick, S. P., and Lindahl, P. A. (2013) Iron Content of *Saccharomyces cerevisiae* Cells Grown under Iron-Deficient and Iron-Overload Conditions. *Biochemistry 52*, 105−114.
(17) Atkinson, A., Khalimonchuk, O., Smith, P., Sabic, H., Eide, D., and Winge, D. R. (2010) Mzm1 Influences a Labile Pool of Mitochondrial Zinc Important for Respiratory Function. *J. Biol. Chem. 285*, 19450−19459.
(18) Theobald, U., Mailinger, W., Baltes, M., Rizzi, M., and Reuss, M. (1997) In vivo analysis of metabolic dynamics in *Saccharomyces cerevisiae*. 1. Experimental observations. *Biotechnol. Bioeng. 55*, 305−316.
(19) Albe, K. R., Butler, M. H., and Wright, B. E. (1990) Cellular Concentrations of Enzymes and their Substrates. *J. Theor. Biol. 143*, 163−195.
(20) Park, J., McCormick, S. P., Chakrabarti, M., and Lindahl, P. A. (2013) Insights into the iron-ome and manganese-ome of Δmtm1 *Saccharomyces cerevisiae* mitochondria. *Metallomics 5*, 656−672.
(21) Ash, D. E. (2004) Structure and function of arginases. *J. Nutr. 134*, 2760s−2764s.
(22) Colleluori, D. M., and Ash, D. E. (2001) Classical and slow-binding inhibitors of human type II arginase. *Biochemistry 40*, 9356−9362.
(23) Costello, L. C., Guan, Z. X., Franklin, R. B., and Feng, P. (2004) Metallothionein can function as a chaperone for zinc uptake transport into prostate and liver mitochondria. *J. Inorg. Biochem. 98*, 664−666.
(24) Caporale, T., Ciavardelli, D., Di Ilio, C., Lanuti, P., Drago, D., and Sensi, S. L. (2009) Ratiometric-pericam-mt, a novel tool to evaluate intramitochondrial zinc. *Exp. Neurol. 218*, 228−234.
(25) Zhang, Y., Lyver, E. R., Knight, S. A. B., Lesuisse, E., and Dancis, A. (2005) Frataxin and mitochondrial carrier proteins, Mrs3p and Mrs4p, cooperate in providing iron for heme synthesis. *J. Biol. Chem. 280*, 19794−19807.
(26) Sensi, S. L., Ton-That, D., Sullivan, P. G., Jonas, E. A., Gee, K. R., Kaczmarek, L. K., and Weiss, J. H. (2003) Modulation of mitochondrial function by endogenous Zn^{2+} pools. *Proc. Natl. Acad. Sci. U.S.A. 100*, 6157−6162.
(27) Park, J. G., Qin, Y., Galati, D. F., and Palmer, A. E. (2012) New sensors for quantitative measurement of mitochondrial Zn^{2+}. *ACS Chem. Biol. 7*, 1636−1640.
(28) McCranor, B. J., Bozym, R. A., Vitolo, M. I., Fierke, C. A., Bambrick, L., Polster, B. M., Fiskum, G., and Thompson, R. B. (2012) Quantitative imaging of mitochondrial and cytosolic free zinc levels in an *in vitro* model of ischemia/reperfusion. *J. Bioenerg. Biomembr. 44*, 253−263.
(29) Costello, L. C., Guan, Z., Franklin, R. B., and Feng, P. (2004) Metallothionein can function as a chaperone for zinc uptake transport into prostate and liver mitochondria. *J. Inorg. Biochem. 98*, 664−666.
(30) Chyan, W., Zhang, D. Y., Lippard, S. J., and Radford, R. J. (2014) Reaction-based fluorescent sensor for investigating mobile Zn^{2+} in mitochondria of healthy versus cancerous prostate cells. *Proc. Natl. Acad. Sci. U.S.A. 111*, 143−148.
(31) Lutz, T., Westermann, B., Neupert, W., and Herrmann, J. M. (2001) The mitochondrial proteins Ssq1 and Jac1 are required for the assembly of iron sulfur clusters in mitochondria. *J. Mol. Biol. 307*, 815−825.
(32) Amutha, B., Gordon, D. M., Gu, Y., Lyver, E. R., Dancis, A., and Pain, D. (2008) GTP is required for iron-sulfur cluster biogenesis in mitochondria. *J. Biol. Chem. 283*, 1362−1371.
(33) Pandey, A., Yoon, H., Lyver, E. R., Dancis, A., and Pain, D. (2012) Identification of a Nfs1p-bound persulfide intermediate in Fe-S cluster synthesis by intact mitochondria. *Mitochondrion 12*, 539−549.
(34) Holmes-Hampton, G. P., Miao, R., Morales, J. G., Guo, Y., Münck, E., and Lindahl, P. A. (2010) A nonheme high-spin ferrous pool in mitochondria isolated from fermenting *Saccharomyces cerevisiae*. *Biochemistry 49*, 4227−4234.
(35) Rauen, U., Springer, A., Weisheit, D., Petrat, F., Korth, H. G., de Groot, H., and Sustmann, R. (2007) Assessment of chelatable mitochondrial iron by using mitochondrion-selective fluorescent iron indicators with different iron-binding affinities. *ChemBioChem 8*, 341−352.
(36) Petrat, F., de Groot, H., Sustmann, R., and Rauen, U. (2002) The chelatable iron pool in living cells: A methodically defined quantity. *Biol. Chem. 383*, 489−502.
(37) Philpott, C. C., and Ryu, M.-S. (2014) Special delivery: Distributing iron in the cytosol of mammalian cells. *Front. Pharmacol. 5* (173), 1−8.
(38) Hider, R. C., and Kong, X. L. (2011) Glutathione: A key component of the cytoplasmic labile iron pool. *BioMetals 24*, 1179−1187.
(39) Li, J. W., and Cowan, J. A. (2015) Glutathione-coordinated [2Fe-2S] cluster: A viable physiological substrate for mitochondrial ABCB7 transport. *Chem. Commun. 51*, 2253−2255.
(40) Cobine, P. A., Ojeda, L. D., Rigby, K. M., and Winge, D. R. (2004) Yeast contain a non-proteinaceous pool of copper in the mitochondrial matrix. *J. Biol. Chem. 279*, 14447−14455.
(41) Cobine, P. A., Pierrel, F., Bestwick, M. L., and Winge, D. R. (2006) Mitochondrial matrix copper complex used in metallation of cytochrome oxidase and superoxide dismutase. *J. Biol. Chem. 281*, 36552−36559.
(42) Cobine, P. A., Pierrel, F., and Winge, D. R. (2006) Copper trafficking to the mitochondrion and assembly of copper metalloenzymes. *Biochim. Biophys. Acta 1763*, 759−772.
(43) Pierrel, F., Cobine, P., and Winge, D. (2007) Metal ion availability in mitochondria. *BioMetals 20*, 675−682.
(44) Dodani, S. C., Leary, S. C., Cobine, P. A., Winge, D. R., and Chang, C. J. (2011) A Targetable Fluorescent Sensor Reveals That Copper-Deficient SCO1 and SCO2 Patient Cells Prioritize Mitochondrial Copper Homeostasis. *J. Am. Chem. Soc. 133*, 8606−8616.
(45) Yang, L., McRae, R., Henary, M. M., Patel, R., Lai, B., Vogt, S., and Fahrni, C. J. (2005) Imaging of the intracellular topography of copper with a fluorescent sensor and by synchrotron X-ray fluorescence microscopy. *Proc. Natl. Acad. Sci. U.S.A. 102*, 11179−11184.
(46) Vest, K. E., Leary, S. C., Winge, D. R., and Cobine, P. A. (2013) Copper Import into the Mitochondrial Matrix in *Saccharomyces cerevisiae* is mediated by Pic2, a mitochondrial carrier family protein. *J. Biol. Chem. 288*, 23884−23892.
(47) Leary, S. C. (2010) Redox regulation of SCO protein function: Controlling copper at a mitochondria crossroad. *Antioxid. Redox Signaling 13*, 1403−1416.
(48) Banerjee, R., Gherasim, C., and Padovani, D. (2009) The tinker, tailor, soldier in intracellular B-12 trafficking. *Curr. Opin. Chem. Biol. 13*, 484−491.
(49) Havemeyer, A., Bittner, F., Wollers, S., Mendel, R., Kunze, T., and Clement, B. (2006) Identification of the missing component in the mitochondrial benzamidoxime prodrug-converting system as a novel molybdenum enzyme. *J. Biol. Chem. 281*, 34796−34802.
(50) Sparacino-Watkins, C. E., Tejero, J., Sun, B., Gauthier, M. C., Thomas, J., Ragireddy, V., Merchant, B. A., Wang, J., Azarov, I., Basu, P., and Gladwin, M. T. (2014) Nitrite reductase and nitric-oxide synthase activity of the mitochondrial molybdopterin enzymes mARC1 and mARC2. *J. Biol. Chem. 289*, 10345−10358.
(51) Hudder, B. N., Morales, J. G., Stubna, A., Münck, E., Hendrich, M. P., and Lindahl, P. A. (2007) Electron paramagnetic resonance and Mössbauer spectroscopy of intact mitochondria from respiring *Saccharomyces cerevisiae*. *JBIC, J. Biol. Inorg. Chem. 12*, 1029−1053.

DOI: 10.1021/bi5015437
Biochemistry 2015, 54, 3442−3453